Influence of the number and distribution of NLS peptides on the photosensitizing activity of multimeric porphyrin–NLS†

Martha Sibrian-Vazquez, Timothy J. Jensen and M. Graça H. Vicente*

Received 21st August 2009, Accepted 25th November 2009
First published as an Advance Article on the web 14th January 2010
DOI: 10.1039/b917280g

Porphyrin–peptide conjugates bearing multiple nuclear localization sequences (NLS) could show increased tumor cell uptake and affinity for nuclear receptors, and consequently increased photodynamic activity. Previous studies suggest that an increase number of NLS might enhance the nuclear uptake of proteins and other macromolecules. We report the syntheses and investigation of a series of multimeric porphyrin–NLS conjugates bearing two, three or four peptides with the minimum sequence PKKKRKV, linked *via* PEG or 5-carbon linkers, and with different distributions at the porphyrin periphery. Our results show that the tumor cell uptake and phototoxicity of these conjugates is mainly determined by their amphiphilic character, and not the number of NLS residues per molecule, contrary to previous studies. The mono- and di-substituted photosensitizers bearing one or two PEG linkers and up to three peptide sequences were found to be the most phototoxic toward human carcinoma HEp2 cells, while the tetra-NLS conjugates symmetrically substituted around the porphyrin ring accumulated the least within cells and were non-phototoxic. All conjugates localized intracellularly within endosomal vesicles and lysosomes, probably as a result of an endocytic mechanism of uptake; as a consequence no nuclear uptake was detected by fluorescence microscopy.

Introduction

The biological efficacy of porphyrin-based sensitizers in the photodynamic therapy (PDT)[1,2] and boron neutron capture therapy (BNCT)[3,4] of tumors depends on their ability for translocation across cellular membranes and delivery into specific organelles within cancer cells. Both PDT and BNCT involve the activation of a tumor-localized sensitizer with either light (in PDT) or low-energy neutrons (in BNCT). The cytotoxic species that ultimately lead to tumor destruction, singlet oxygen and other reactive oxygen species (ROS) in PDT, and the high linear energy particles (high-LET) $^{4}He^{2+}$ and $^{7}Li^{3+}$ in BNCT, have limited travel distances in tissues (~1 μm for $^{1}O_2$, 5 μm for $^{4}He^{2+}$ and 9 μm for $^{7}Li^{3+}$) and therefore their sites of generation determine the therapeutic outcome of these cancer treatments.[1–5] Several strategies have been investigated in order to improve the biological efficacy of first and second generation PDT photosensitizers, such as purified hematoporphyrin derivative, monoaspartyl-chlorin e_6 and *meso*-tetra(3-hydroxyphenyl)chlorin, including their PEGylation and/or conjugation to monoclonal antibodies, proteins, peptides and oligonucleotides.[6–8] In particular the conjugation of porphyrin photosensitizers to peptide sequences bearing specific targeting properties, for example the use of nuclear localization sequences (NLS), is well documented due to the ease of peptide synthesis and their structural modification. NLS are known to mediate protein import into the cell nucleus, an important target in both PDT and BNCT. For example, although ~30 μg boron per g of tumor are calculated to be required for effective BNCT, about 50% less boron is needed for effective lethal damage if it locates intracellularly as opposed to extracellularly, and this amount can be further reduced by a factor of 2 to 5 if the boron localizes inside or in close proximity to the cell nucleus.[5] NLS peptides generally contain a cluster of at least four cationic amino acids (lysine and/or arginine), often flanked by proline or glycine.[9,10] Among these, the NLS of the simian virus (SV40) large T antigen with minimum sequence PKKKRKV has been extensively studied.[11–14] Previous investigations have shown that the conjugation of porphyrin-based photosensitizers to one or more NLS significantly increases their photosensitizing activity, possibly as a consequence of nuclear delivery and subsequent nucleic acid photodamage. Examples of such studies include the conjugation of a peptide sequence containing an encoded NLS to a Mn(III)-porphyrin,[15] and the conjugation of chlorin-e_6 to peptide shuttles containing multiple SV40 NLS[16] or to proteins containing the SV40 NLS.[17–20] We have previously investigated the cellular properties of mono-functionalized *meso*-tetraphenylporphyrins bearing either one or two SV40 NLS peptides linked to the porphyrin *via* a low molecular weight PEG spacer.[21–23] These studies suggest that the nature and number of NLS and of PEG groups at the porphyrin periphery significantly influence the chemical and biological properties of the photosensitizer, as they alter the preferential conformations, aggregation behavior and hydrophobic character of the conjugates.[21–24] In the present study we further investigate the effect of the number of NLS with minimum sequence PKKKRKV, their distribution at the porphyrin periphery and nature of the linker on the cellular uptake and photosensitizing properties of the resulting porphyrin–peptide conjugates. We report for the first time the synthesis and

Department of Chemistry, Louisiana State University, Baton Rouge, LA, 70803, USA. E-mail: vicente@lsu.edu; Fax: +1 225 578 3458; Tel: +1 225 578 7405

† Electronic supplementary information (ESI) available: Proton-NMR spectra for porphyrin–NLS conjugates **4**, **6**, **8**, **9** and **10** and HPLC traces for porphyrin–NLS conjugates **4**, **8** and **9**. See DOI: 10.1039/b917280g

investigations of new di-, tri- and tetra-substituted porphyrin–NLS conjugates (**6**, **8**, **9** and **10**), and of a new porphyrin containing a single peptide sequence bearing three consecutive NLS (**4**). These multimeric NLS conjugates could potentially show increased binding affinity to nuclear receptors, promote sensitizer tumor cell uptake, enhance photodynamic activity and overall PDT and BNCT efficacy. Our biological studies conducted on human carcinoma HEp2 cells suggest that an amphiphilic conjugate containing a single peptide sequence bearing multiple NLS is the most promising approach at increasing porphyrin delivery to tumor cells and conjugate phototoxicity; multiple NLS symmetrically distributed at the porphyrin periphery tend to reduce conjugate uptake and phototoxicity, in part as a result of decreased conjugate amphiphilicity and increased hydrophilicity.

Results and discussion

Synthesis

The biological efficacy of porphyrin-based sensitizers could be increased upon their conjugation to one or more peptides that enhance their tumor cell uptake and delivery into sensitive intracellular compartments, such as the nuclei. We have previously reported that a porphyrin–monoNLS bearing a low molecular weight PEG spacer efficiently accumulated within human carcinoma HEp2 cells and it was highly phototoxic.[21] In the present study we investigated a new series of multimeric porphyrin–NLS conjugates (**3**, **4**, **6**, **8**, **9** and **10**) containing between two and four peptides with the sequence PKKKRKV, the minimum identified as required for promoting transport into the cell nucleus.[11-13] The peptides were introduced at different positions around the porphyrin ring and were linked *via* either a low molecular weight PEG (in conjugates **3**, **4**, **6**, and **10**) or a five-carbon spacer (in conjugates **8** and **9**) to minimize interactions with the porphyrin moiety.[21,26] This series of multimeric porphyrin–NLS was synthesized *via* amide bond formation, using either solution or solid-phase synthetic methodologies, as shown in Schemes 1–3. Mono-, di- and tetra-(4-aminophenyl)porphyrin derivatives were used as the photosensitizer platform, because amino-substituted porphyrins are readily available[25] and the amino groups can be quantitatively converted into carboxylates upon reaction with diglycolic or glutaric anhydrides.[23,26] The di-carboxylate branch in porphyrin **2** was introduced by coupling porphyrin **1** with di-Boc protected aspartic acid in the presence of HOBt and EDCI, followed by deprotection using TFA.[24] The low molecular weight PEG linkers in conjugates **3**, **4**, **6** and **10** were introduced *via* the coupling to $NH_2CH_2CH_2(OCH_2CH_2)_5CH_2CO_2{}^tBu$ using HOBt, TBTU and EDCI as the activating agents,[23] deprotection with TFA and conjugation to the free N-terminus of the protected peptides, either *via* a glycine (in conjugates **3**, **6**, and **10**) or aspartate (in conjugate **4**) residue. After deprotection (and cleavage from the solid support in the case of **4**) using a mixture containing TFA–H_2O–TIS–phenol, the porphyrin–peptide conjugates were purified by HPLC and isolated in 29–53% yields. The linear peptide DPKKKRKVDPKKKRKVDPKKKRKV used in the solid-phase synthesis of conjugate **4** is encoded in an expression vector commercially available (pShooter™) that targets a recombinant protein to the nucleus of mammalian cells. Since this linear tri-NLS peptide contains aspartic acid residues as the linking units between the NLS sequences, it includes three additional negative charges compared with the other conjugates.

All porphyrin–NLS conjugates were soluble in DMF, DMSO, and water, and were characterized by NMR, MS and UV-Vis. Conformational studies on the SV40 NLS peptides conjugated to the porphyrins were conducted in a membrane-mimicking environment consisting of 10% (v/v) TFE–water at pH 7.00. As shown in Fig. 1 all porphyrin–peptide conjugates exhibit negative Cotton effects at 198–207 nm, which are characteristic of a random coil conformation. For example for polylysine at pH 7, $[\theta] = -41\,900$ deg cm^2 dmol^{-1} at 197 nm.[27] Such a conformation is in agreement with a previous report based on the crystal structure of the protein kariopherin α/SV40,[28] where the peptide sequence adopts an extended random coil conformation, probably due to the electrostatic repulsion between the positively charged residues.

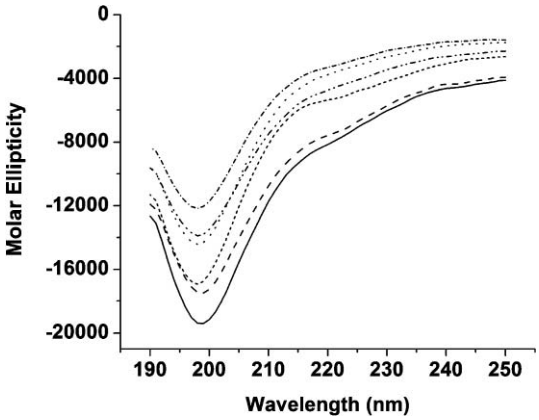

Fig. 1 CD spectra in the amide region of porphyrin peptide conjugates: **3** (full line), **4** (short dash line), **6** (dash line), **8** (dash–dot–dot–dash line), **9** (dot–dash line), **10** (dot line), in TFE–H_2O at pH 7.00. Conjugate concentration 20 μM. The ellipticity is given in deg cm^2 dmol^{-1}, cell path was 0.1 cm, temperature 25 °C.

Cellular studies

The uptake of the conjugates by human HEp2 cells was found to be dependent on the number and distribution of the NLS residues at the porphyrin periphery, and on the nature of the linker, as shown in Fig. 2. The tetra-NLS conjugate **10** bearing four PEG linkers was by far the least accumulated within cells of all conjugates studied, probably due to its high hydrophilicity and tendency towards aggregation, as we have previously observed for the corresponding porphyrin–$(PEG)_4$ precursor.[24] In contrast, the tetra-NLS conjugate **8** containing four 5-carbon spacers in place of the PEG linkers in **10** accumulated four times more than conjugate **10**, demonstrating for the first time the importance of the nature of the linkers in this type of multimeric peptide–sensitizer conjugate. Furthermore, the tri-NLS conjugate **9** bearing 5-carbon spacers was taken up faster and to a higher extent than the tetra-NLS **8**, probably due to its higher amphiphilicity, indicating that an increasing number of NLS residues at the porphyrin periphery might not lead to increased cellular uptake and phototoxicity (*vide infra*). Our results show that, in fact, all asymmetric conjugates were taken up to a higher extent than the symmetric tetra-NLS conjugates **8** and **10**. The asymmetric substitution at the

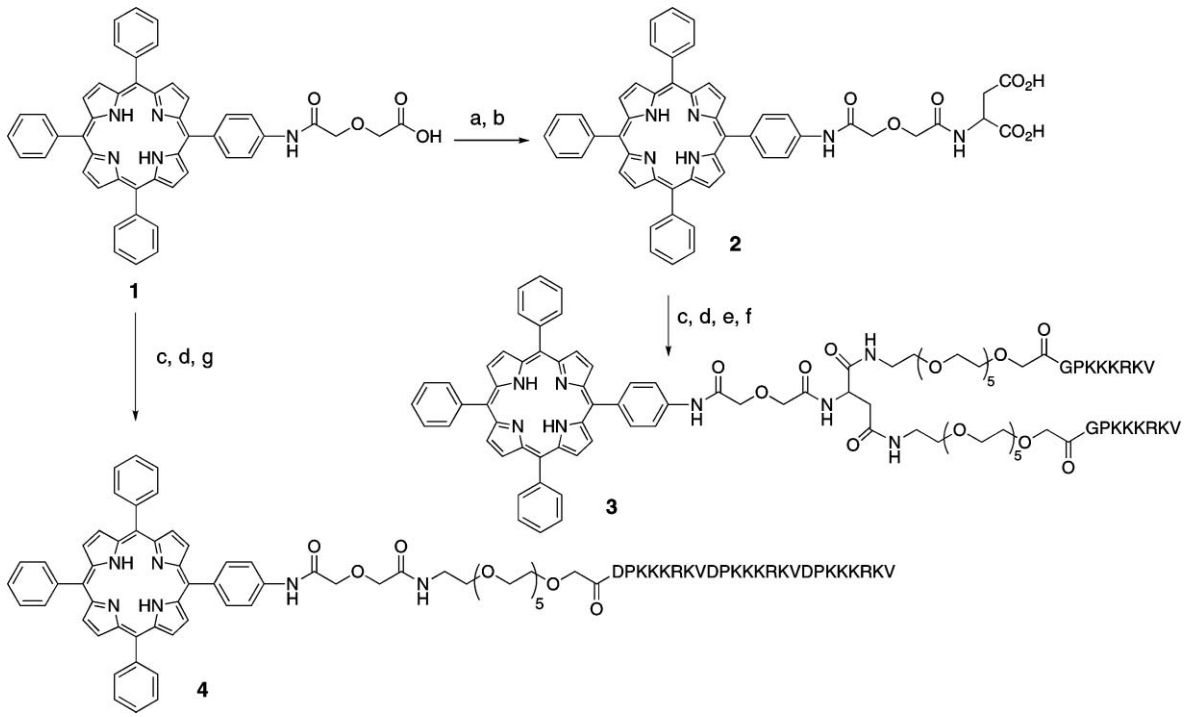

Scheme 1 *Conditions*: (a) Et_3N, DMAP, HOBt, aspartic acid di(*tert*-butyl)ester hydrochloride, EDCI, DMF, rt, 48 h (98%). (b) TFA, rt, 4 h (98%). (c) DIEA, HOBt, TBTU, $NH_2CH_2CH_2(OCH_2CH_2)_5OCH_2CO_2{}^tBu$, DMF, rt, 48 h (59%). (d) TFA, CH_2Cl_2, rt, 4 h (98%). (e) Et_3N, HOBt, DMAP, HGlyProLys(Boc)Lys(Boc)Lys(Boc)Arg(Pbf)Lys(Boc)Val(O^{t}Bu), DMF, rt, 48 h (48%). (f) TFA–TIS–H_2O–phenol 88 : 2 : 5 : 5, rt, 4 h (95%). (g) HOBt, TBTU, DIEA, NH_2-peptidyl-PAL-PEG-PS resin, rt, 48 h, then TFA–TIS–H_2O–phenol 88 : 2 : 5 : 5, rt, 4 h (53%).

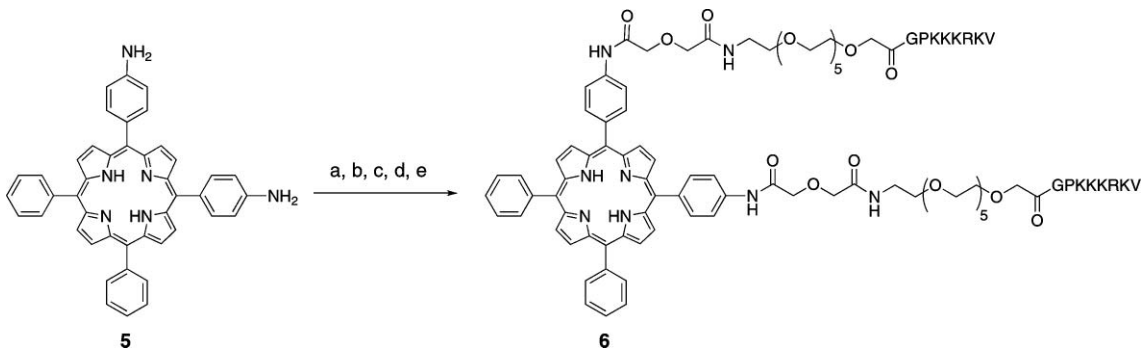

Scheme 2 *Conditions*: (a) diglycolic anhydride, DMF, rt, 24 h (99%). (b) Et_3N, DMAP, HOBt, EDCI, $NH_2CH_2CH_2(OCH_2CH_2)_5OCH_2CO_2{}^tBu$, DMF, rt, 48 h (35%). (c) TFA, rt, 4 h (95%). (d) Et_3N, HOBt, DMAP, EDCI, HGlyProLys(Boc)Lys(Boc)Lys(Boc)Arg(Pbf)Lys(Boc)Val(O^{t}Bu), DMF, rt, 48 h (38%). (e) TFA–TIS–H_2O–phenol 88 : 2 : 5 : 5, rt, 4 h (97%).

photosensitizer periphery confers amphiphilicity on the molecules, which deeply influences their biological efficacy.

While the tri-NLS conjugate **9** was the most taken up by cells at short time points (less than 4 h), after >8 h, conjugate **4** containing three NLS in a linear sequence showed the highest cellular uptake of all conjugates studied (see also Figure S2 in the ESI†). Furthermore, the mono-substituted photosensitizer bearing a branched di-NLS, *i.e.* conjugate **3**, was taken up to a higher extent than the di-NLS conjugate **6** at all time points investigated, indicating that the distribution of the NLS residues about the photosensitizer moiety and the resulting conjugate amphiphilicity play an important role in determining the extent of their cellular uptake. These results are in agreement with previous studies suggesting that the number and distribution of hydrophilic groups at the porphyrin periphery and photosensitizer amphiphilicity are important for enhancing translocation across plasma membranes, *e.g.*[24,29] In particular, the amphiphilicity conferred by mono-substitution of the tetraphenylporphyrin macrocycle, as in **3** and **4**, might enhance the affinity of these conjugates for lipid/aqueous interfaces, therefore favoring cellular uptake.

Conjugate **4**, the most taken up by cells at >8 h, was also the most toxic showing IC_{50} (dark) = 30 μM and IC_{50} (light, 0.5 J cm^{-2}) = 4.9 μM, as shown in Fig. 3 and 4, respectively. All other conjugates were either non-toxic in the dark at concentrations up to 100 μM or mildly toxic (IC_{50} = 98 μM for conjugate **9**) to HEp2 cells. The di-NLS conjugates **3** and **6** were also found to be phototoxic, showing IC_{50} (light, 0.5 J cm^{-2}) of 9.3 and 8.7 μM, respectively. It is possible that the superior phototoxicity observed

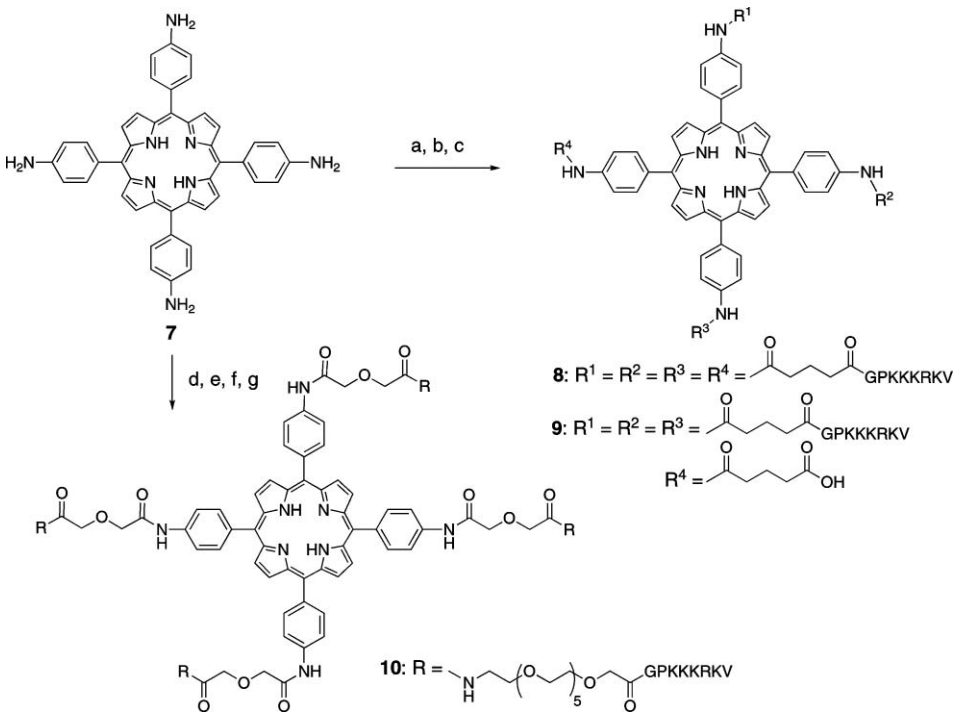

Scheme 3 *Conditions*: (a) glutaric anhydride, DMF, rt, 24 h (100%). (b) Et_3N, HOBt, DMAP, EDCI, HGlyProLys(Boc)Lys(Boc)Lys(Boc)Arg(Pbf)-Lys(Boc)Val(O^{t}Bu), rt, 48 h (32%). (c) TFA–TIS–H_2O–phenol 88 : 2 : 5 : 5, rt, 4 h (90%). (d) Glycolic anhydride then DIEA, HOBt, TBTU, $NH_2CH_2CH_2(OCH_2CH_2)_5OCH_2CO_2{}^t$Bu, DMF rt, 48 h (40%). (e) TFA, DCM, rt, 4 h (98%). (f) Et_3N, HOBt, DMAP, EDCI, HGlyPro-Lys(Boc)Lys(Boc)Lys(Boc)Arg(Pbf)Lys(Boc)Val(OtBu), DMF, rt, 48 h (52%). (g) TFA–TIS–H_2O–phenol 88 : 2 : 5 : 5, rt, 4 h (86%).

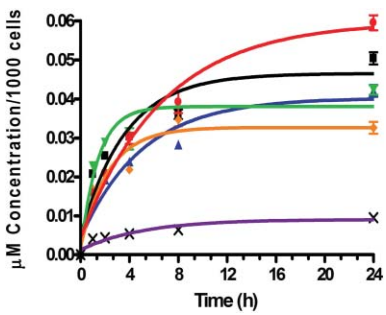

Fig. 2 Time-dependent uptake of porphyrin–NLS conjugates **3** (black), **4** (red), **6** (blue), **8** (orange), **9** (green), and **10** (purple) at 10 µM by HEp2 cells.

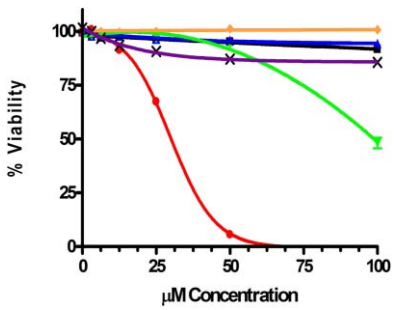

Fig. 3 Dark toxicity of porphyrin–NLS conjugates **3** (black), **4** (red), **6** (blue), **8** (orange), **9** (green), and **10** (purple) toward HEp2 cells using the Cell Titer Blue assay.

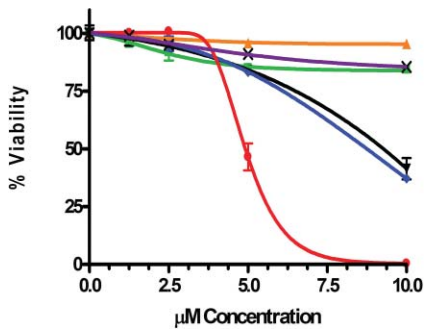

Fig. 4 Phototoxicity of porphyrin–NLS conjugates **3** (black), **4** (red), **6** (blue), **8** (orange), **9** (green), and **10** (purple) toward HEp2 cells using 0.5 J cm^{-2} dose light.

for conjugates **3**, **4** and **6** might be a consequence of their higher cellular uptake.

The subcellular localization of all conjugates was investigated in HEp2 cells using fluorescence microscopy and the patterns observed, as well as their overlay with those of the organelle specific fluorescent probes LysoSensor Green (lysosomes), MitoTracker Green (mitochondria), and $DiOC_6$ or ERtracker Blue-White (ER), are shown in Fig. 5–10. All conjugates were found to collect mainly in large vesicles as shown by the punctuate patterns observed in Fig. 5B–10B, some of which co-localized with the cell lysosomes (Fig. 5F–10F), therefore there was no observed correlation between the preferential sites of localization and PDT efficacy.

Although these molecules contain multiple NLS, the cell nucleus was not observed to be a site of intracellular localization. This

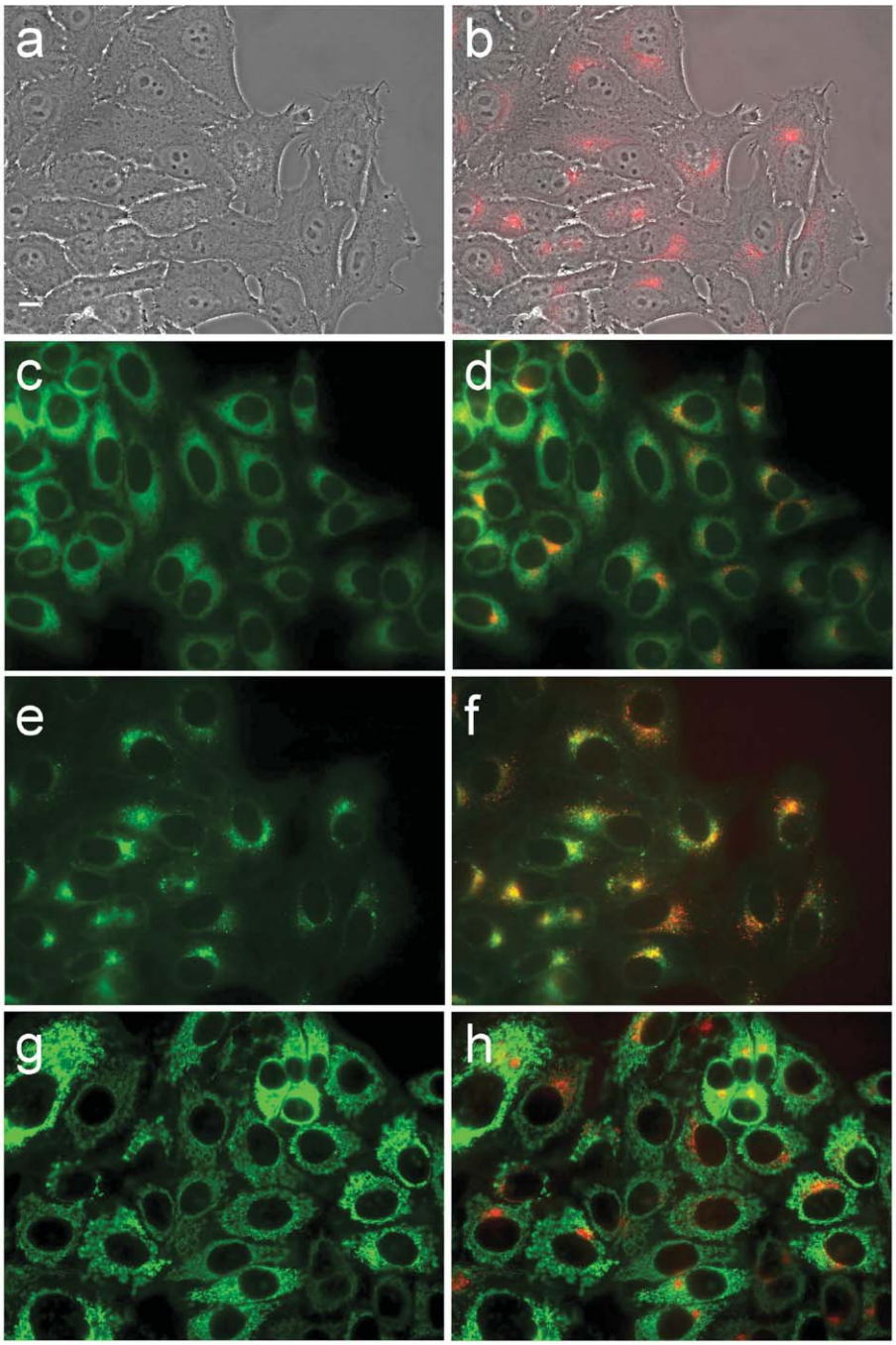

Fig. 5 Subcellular localization of conjugate **3** in HEp2 cells at 10 μM for 24 h. (a) Phase contrast, (b) overlay of **3** fluorescence and phase contrast, (c) $DiOC_6$ fluorescence, (e) LysoSensor Green fluorescence, (g) MitoTracker Green fluorescence, (d), (f), (h), overlays of organelle tracers with porphyrin **3** fluorescence. Scale bar: 10 μm.

result might reflect a preference for an endocytic mechanism of cell internalization for this type of conjugate, favoring their localization within endosomal vesicles, some of which might fuse with the cell lysosomes. As a consequence, most of the conjugates stay trapped within endosomes and lysosomes where the peptide sequences are slowly degraded, as we have previously reported.[22] The inefficient cytoplasmic delivery of drugs conjugated to a variety of carriers (*e.g.* liposomes, polymers and peptides) as a consequence of an endocytic internalization is a well documented phenomenon.[30] It is however possible that a small amount of the phototoxic multi-NLS conjugates **3**, **4** and **6** might be able to escape the vesicular compartments with one or more NLS intact and reach the nucleus, thus explaining their higher phototoxicity.

Our results are in agreement with previously studies[21–24,31] showing that the amount of photosensitizer accumulated within target cells and its subcellular distribution determine its toxicity and biological efficacy. Other studies have shown that the number and distribution of SV40 large T antigen NLS residues on

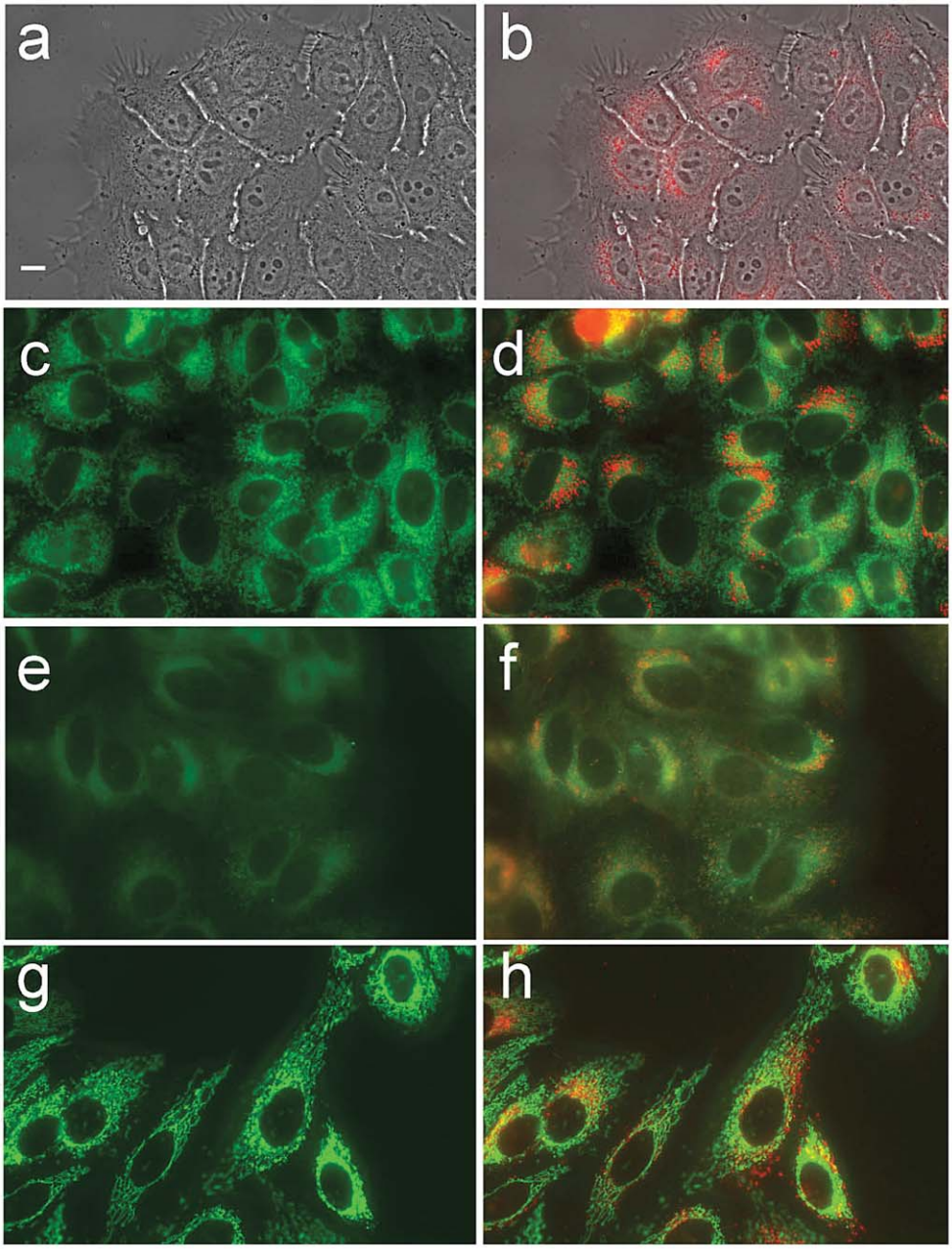

Fig. 6 Subcellular localization of conjugate **4** in HEp2 cells at 10 μM for 24 h. (a) Phase contrast, (b) overlay of **4** fluorescence and phase contrast, (c) $DiOC_6$ fluorescence, (e) LysoSensor Green fluorescence, (g) MitoTracker Green fluorescence, (d), (f), (h), overlays of organelle tracers with porphyrin **4** fluorescence. Scale bar: 10 μm.

proteins and other macromolecules play an important role on their interaction with nuclear receptors and transport, and in general nuclear uptake increases with the number of NLS per molecule.[16,19,30,32] For example, chlorin e_6 conjugates containing BSA, insulin and multiple NLS residues were shown to have up to a 2000-fold increase in phototoxicity compared with free chlorin e_6.[19] In another study, chlorin e_6 was conjugated to either one linear SV40 NLS followed by a pentalysine cytoplasmic translocation signal (CTS) peptide, or to a lysine-based branched construct (so-called "loligomer") bearing eight identical arms composed of a chlorin e_6 molecule conjugated to a linear NLS and CTS sequence.[16]

Both conjugates showed enhanced photodynamic activity compared with free chlorin e_6, and the extent of nuclear uptake was only significant for the chlorin e_6–loligomer containing eight SV40 NLS after release from endocytic vesicles, presumably favored due to the presence of the polylysine scaffold in the loligomer. Other studies conducted on multimeric RGD-containing molecules have shown that integrin receptor binding affinity in general increases with the number of RGD peptides in the molecule.[33–38] For example, the integrin binding affinity and tumor cell uptake of a series of conjugates bearing up to eight RGD tripeptides and labeled with a near-IR fluorophore were shown to be dependent on both the number of RGD moieties and their spatial arrangement;[33]

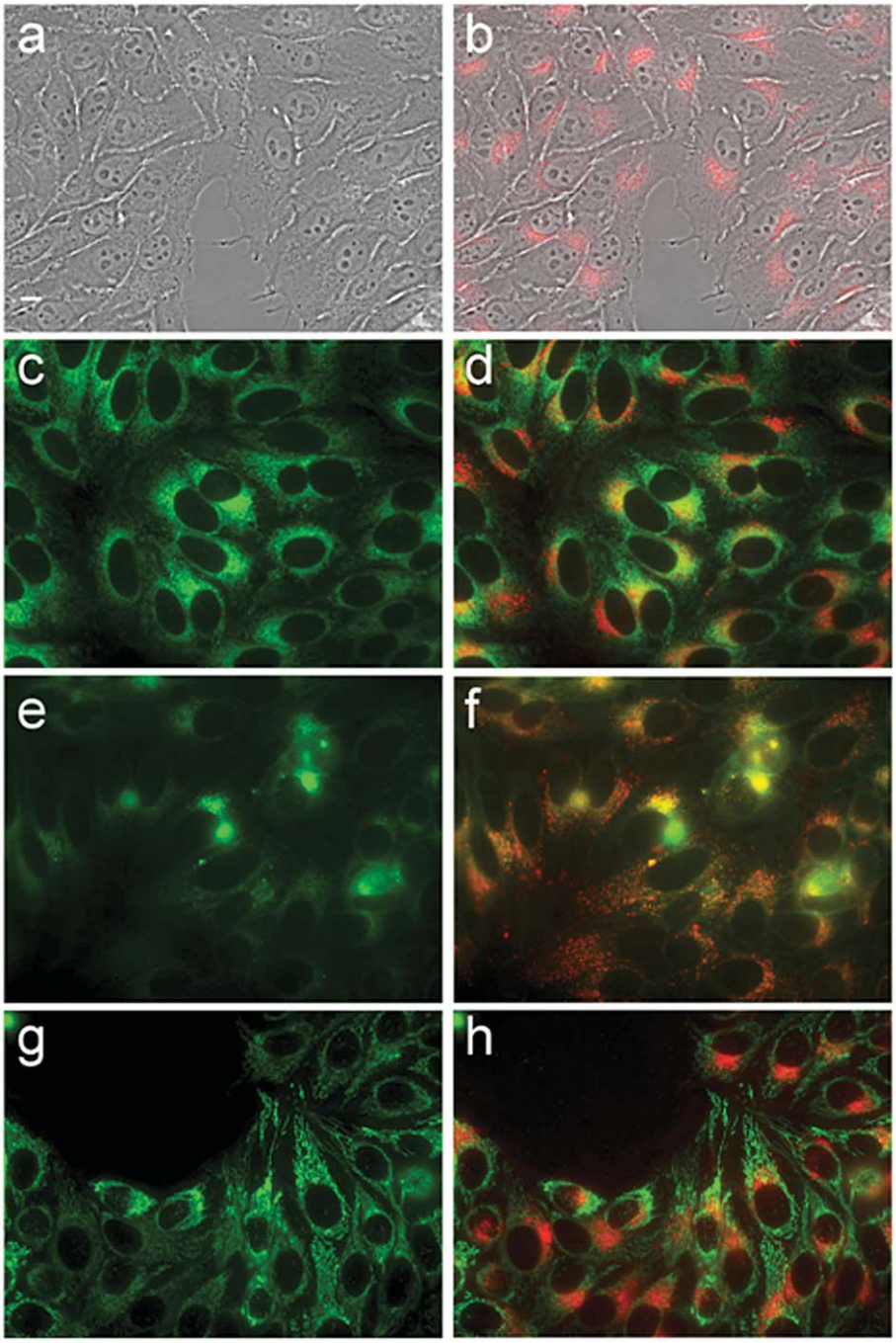

Fig. 7 Subcellular localization of conjugate **6** in HEp2 cells at 10 μM for 24 h. (a) Phase contrast, (b) overlay of **6** fluorescence and phase contrast, (c) $DiOC_6$ fluorescence, (e) LysoSensor Green fluorescence, (g) MitoTracker Green fluorescence, (d), (f), (h), overlays of organelle tracers with conjugate **6** fluorescence. Scale bar: 10 μm.

an increase in integrin binding affinity and cellular internalization was observed *in vitro* with increasing number of RGD units in the molecule, while *in vivo* most multi-RGD compounds showed similar tumor uptake after 24 h, although molecules with higher receptor binding affinity localized faster in the target tumor. Other studies have reported enhanced integrin binding affinity and cellular uptake of conjugates containing multi-RGD residues coupled to a polymer,[34] protein,[35] peptide,[36] fluorophore[37] and a dendrimer.[38] While the targeting of cell surface receptors, such as integrin receptors, seems to increase with increasing number of ligand peptides, *i.e.* RGD residues, in the molecule, the specific subcellular delivery of drugs also depends on their cytoplasmic delivery and trafficking.

Conclusions

A series of multimeric porphyrin–NLS conjugates containing between two and four SV40 large T antigen NLS peptides with

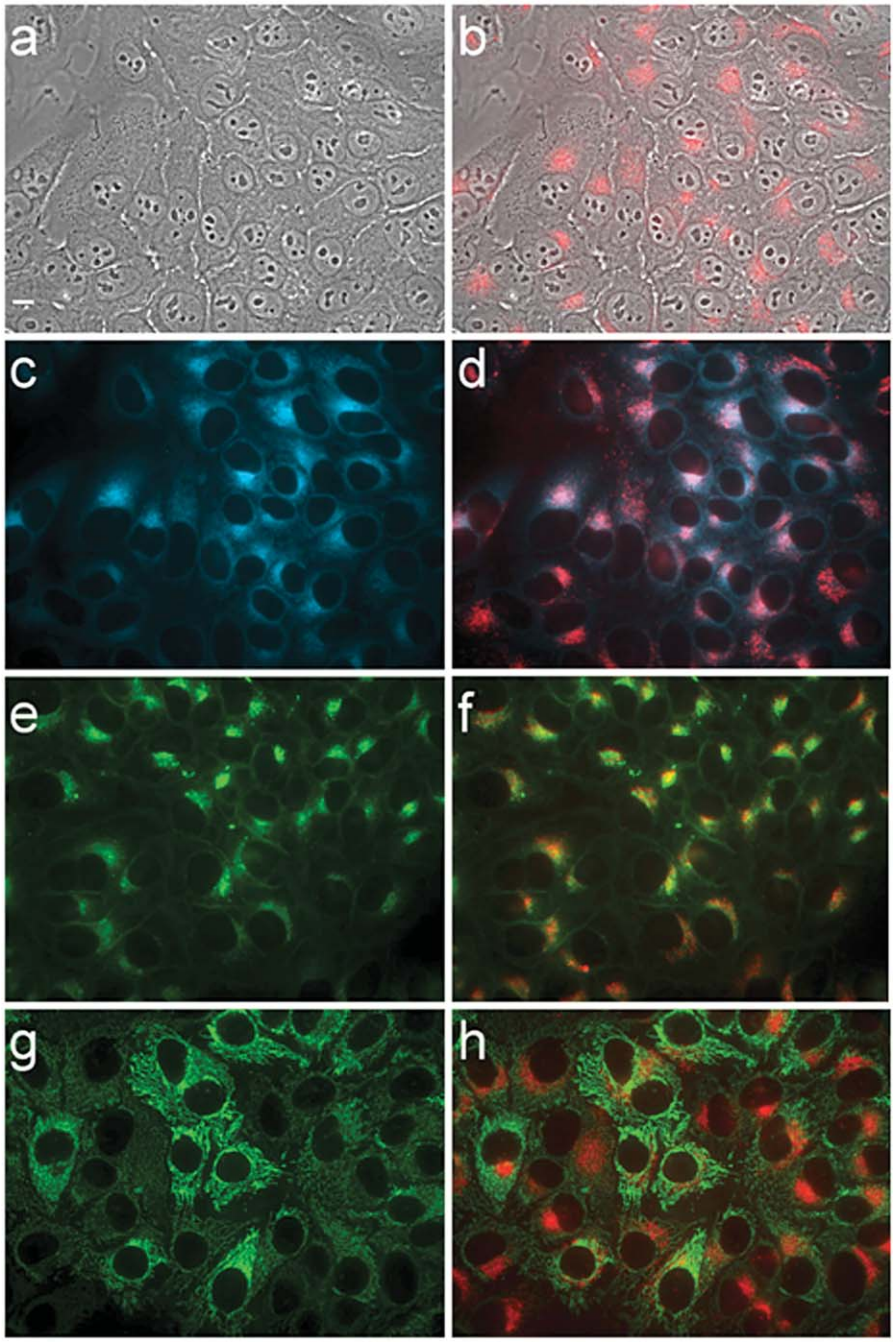

Fig. 8 Subcellular localization of conjugate **8** in HEp2 cells at 10 μM for 24 h. (a) Phase contrast, (b) overlay of **8** fluorescence and phase contrast, (c) ER Tracker Blue-White fluorescence, (e) LysoSensor Green fluorescence, (g) MitoTracker Green fluorescence, (d), (f), (h), overlays of organelle tracers with conjugate **8** fluorescence. Scale bar: 10 μm.

the minimum sequence PKKKRKV, linked *via* PEG or 5-carbon spacers, and with different distributions around the porphyrin ring were synthesized using solution- or solid-phase techniques. NLS mediate protein import into the cell nucleus, an important target in both PDT and BNCT. In all compounds the peptide sequences adopt an extended random coil conformation, as expected for such hydrophilic peptides. The uptake of these conjugates by human carcinoma HEp2 cells and their phototoxicity was found to be dependent on the number and distribution of the NLS at the porphyrin periphery, and the nature of the linker. The highest uptake and phototoxicity were observed for porphyrin–$(NLS)_3$ **4** bearing a single linear sequence containing three consecutive NLS linked *via* a low molecular weight PEG group to the porphyrin ring, maybe as a result of its amphiphilicity. More than three NLS, *i.e.* four NLS, symmetrically distributed at the porphyrin periphery, significantly decreased cellular uptake and phototoxicity, maybe as a result of increased hydrophilicity. All multimeric porphyrin–NLS were found to remain trapped within endosomal vesicles and lysosomes, probably as a result of an endocytic mechanism of uptake. The inefficient cytoplasmic delivery of these conjugates might

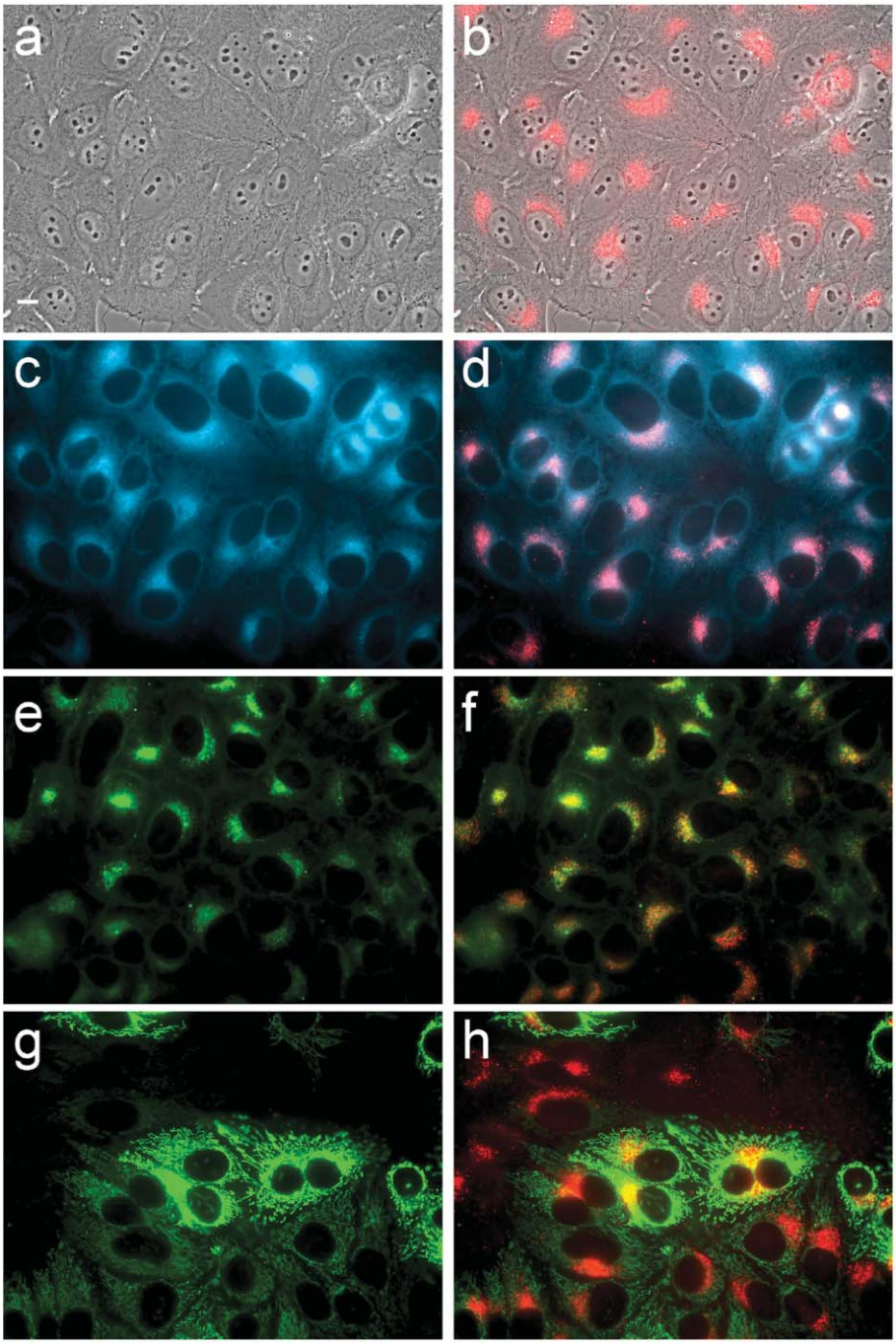

Fig. 9 Subcellular localization of conjugate **9** in HEp2 cells at 10 μM for 24 h. (a) Phase contrast, (b) overlay of **9** fluorescence and phase contrast, (c) ER Tracker Blue-White fluorescence, (e) LysoSensor Green fluorescence, (g) MitoTracker Green fluorescence, (d), (f), (h), overlays of organelle tracers with conjugate **9** fluorescence. Scale bar: 10 μm.

be responsible for their observed low phototoxicities. Overall, our results show that the cellular uptake and phototoxicity of porphyrin–peptide conjugates strongly depend on the distribution of the targeting peptide sequences at the porphyrin periphery. Unlike previous reports, our results show that an increased number of NLS residues at the periphery of a porphyrin does not necessary increase the tumor cell uptake and photodynamic activity of peptide-containing porphyrin photosensitizers. Our studies provide a template for the design of effective amphiphilic porphyrin–peptide conjugates for the detection and treatment of cancer.

Experimental section

Chemistry

Unless otherwise indicated, all commercially available starting materials were used directly without further purification. All

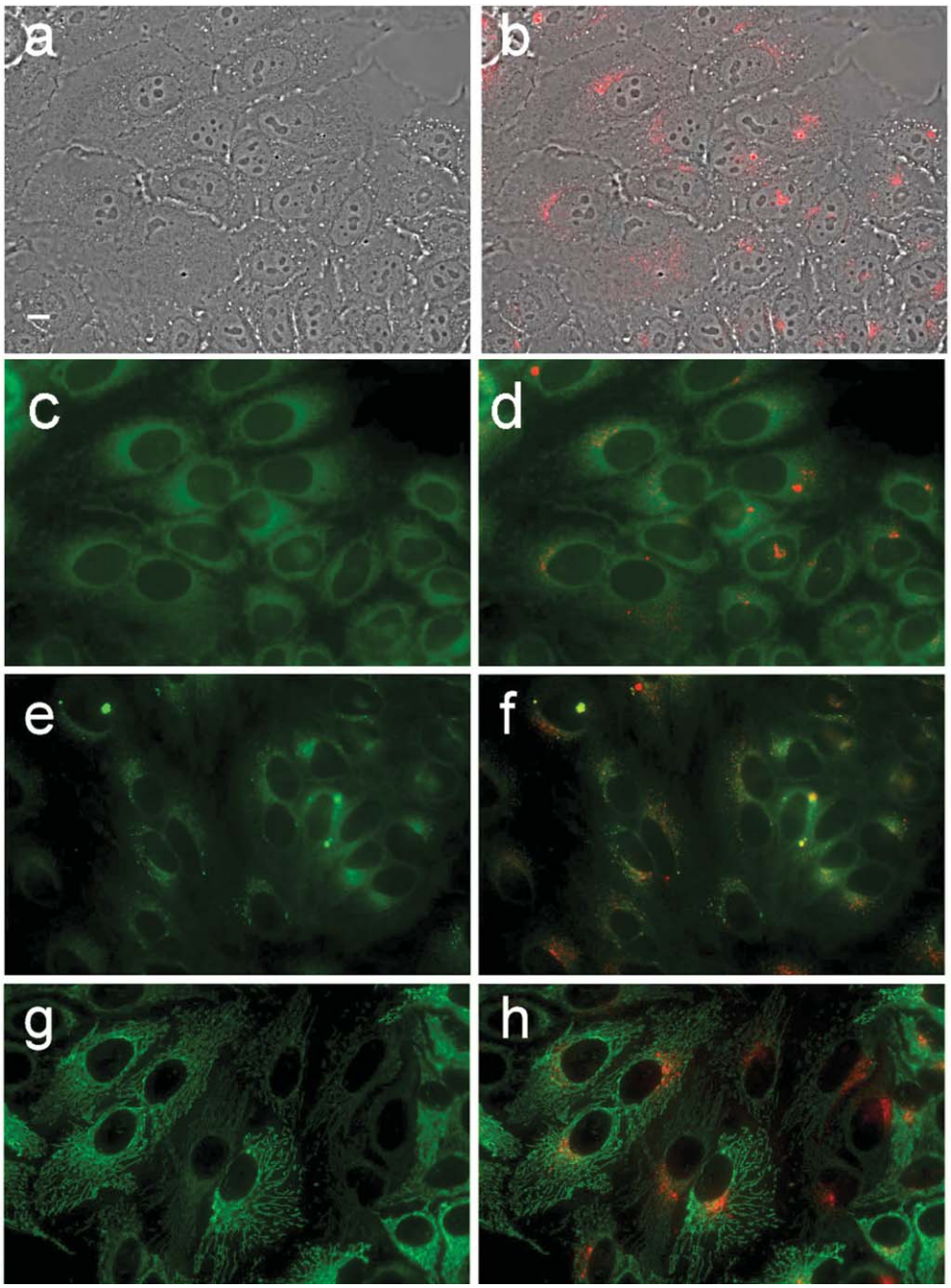

Fig. 10 Subcellular localization of conjugate **10** in HEp2 cells at 10 μM for 24 h. (a) Phase contrast, (b) overlay of conjugate **10** fluorescence and phase contrast, (c) $DiOC_6$ fluorescence, (e) LysoSensor Green fluorescence, (g) MitoTracker Green fluorescence, (d), (f), (h), overlays of organelle tracers with conjugate **10** fluorescence. Scale bar: 10 μm.

reactions were monitored by TLC using Sorbent Technologies 0.25 mm silica gel plates with or without UV indicator (60F-254). Silica gel (Sorbent Technologies 32-63 μm) was used for flash column chromatography. ^{1}H NMR spectra were obtained on a ARX-300 Bruker spectrometer. Chemical shifts (δ) are given in ppm relative to d_6-DMSO or $CDCl_3$ (2.49 and 7.26 ppm, respectively). Electronic absorption spectra were measured on a Perkin Elmer Lambda 35 UV-Vis spectrophotometer. Mass spectra were obtained on an Applied Biosystems QSTAR XL, a hybrid QqTOF mass spectrometer with a MALDI ionization source using CCA as the matrix. HPLC separation and analysis were carried out on a Dionex system including a P680 pump and a UVD340U detector. Semi-preparative HPLC was carried out using a Luna C_{18} 100 Å, 5 μm, 10 × 250 mm (Phenomenex, USA) column and a stepwise gradient; analytical HPLC was carried out using a Delta Pak C_{18} 300 Å, 5 μm, 3.9 × 150 mm (Waters, USA) column and a stepwise gradient. 5,10,15,20-Tetra(*p*-aminophenyl)porphyrin **7** was purchased from Frontier Sci. The syntheses of porphyrins **1**[21] and **5**,[25] and of porphyrin–NLS conjugate **3**[23] were performed as previously described. The HPLC traces and

^{1}H-NMR spectra for the porphyrin–NLS conjugates are given in the ESI.†

Porphyrin–NLS 4. The peptide sequence DPKKKRKVDP-KKKRKVDPKKKRKV was prepared on an automated peptide synthesizer (Applied Biosystems Pioneer, Peptide Synthesis System, USA) in a 0.2 mmol scale, using the Fmoc strategy of solid-phase peptide synthesis. A 4-fold excess of the Fmoc-protected amino acids were coupled to the PAL-PEG-PS resin using HOBt/TBTU as the activating agents. Conjugation to the porphyrin precursor (0.05 mmol) was achieved using the same methodology as we have previously described.[21–23] The purification of the porphyrin conjugate **4** was performed by reverse phase HPLC on a Luna C_{18} semi-preparative column (10 × 250 mm, 5 μm) using a solvent system of water–acetonitrile both containing 0.1% TFA, with a stepwise gradient from 20 to 95%. The fraction containing this conjugate was collected and lyophilized to yield 0.053 g (53%) of pure conjugate. The purity of the peptide was >98% as determined by HPLC on an analytical Delta Pak C_{18} (3.9 × 150 mm, 5 μm) column, $t_r = 9.92$ min. ^{1}H NMR (d_6-DMSO, 300 MHz): δ 10.51 (1H, s), 8.83 (9H, s), 8.44 (2H, s), 7.82–8.22 (18H, m), 7.11–7.55 (12H, m), 4.79 (3H, s, br), 4.20 (30H, s, br), 3.46–3.68 (90H, m), 3.06 (6H, s), 2.74 (30H, s), 1.29–1.85 (84H, m), 0.79 (18H, s), –2.91 (2H, s). MS (MALDI) m/z 4001.176 (M + H$^+$) calculated for $C_{194}H_{306}N_{52}O_{40}$ 4004.3510.

Porphyrin–NLS 6. To a solution of 5,10-di(*p*-aminophenyl)-diphenylporphyrin **5** (0.020 g, 0.031 mmol) in 500 μL of DMF was added diglycolic anhydride (0.011 g, 0.093 mmol). The reaction mixture was stirred at room temperature for 48 h and then diluted with 5 mL of chloroform. The resulting porphyrin was precipitated by addition of hexanes, filtered and washed with warm water to remove unreacted diglycolic anhydride, and dried under vacuum to give a green solid (0.027 g, 99%). UV-Vis ($CHCl_3$) λ_{max} (ε/M^{-1}cm^{-1}) 421 (281 400), 517 (17 600), 553 (11 000), 591 (6700), 648 (5700). ^{1}H NMR (MeOD, 300 MHz): δ 8.84–8.91 (8H, m), 8.20–8.25 (8H, m), 8.09–8.12 (4H, m), 7.79–7.86 (8H, m), 4.42 (8H, s). HRMS (MALDI) m/z 877.3001 (M + H$^+$), calculated for $C_{52}H_{40}N_6O_8$ 877.2908. The dicarboxylate porphyrin intermediate (0.030 g, 0.035 mmol) was dissolved in 600 μL of DMF. To this solution were added in the following order: DIEA (0.036 g, 0.278 mmol), HOBt (0.0344 g, 0.087 mmol), TBTU (0.028 g, 0.087 mmol), and $NH_2CH_2CH_2(OCH_2CH_2)_5CH_2CO_2{}^tBu$ (0.034 g, 0.087 mmol). The reaction mixture was stirred at room temperature for 48 h and then diluted with ethyl acetate (20 mL). The organic phase was washed with water (2 × 20 mL), saturated $NaHCO_3$ (2 × 20 mL), water (2 × 20 mL), and then dried over anhydrous Na_2SO_4, filtered, and the solvent evaporated under vacuum to leave a purple residue. The resulting dipegylated porphyrin was isolated by flash chromatography on silica gel using $CHCl_3$–MeOH 90 : 10 for elution, giving 0.013 g, 35% yield. UV-Vis ($CHCl_3$) λ_{max} (ε/M^{-1}cm^{-1}) 421 (295 300), 516 (15 600), 553 (10 400), 591 (7200), 646 (6 300). ^{1}H NMR ($CDCl_3$, 300 MHz): δ 8.84–8.92 (8H, m), 8.18–8.23 (8H, m), 8.09–8.13 (4H, m), 7.75–7.77 (8H, m), 7.55 (2H, s), 4.37 (4H, s), 4.30 (4H, s), 3.99 (4H, s), 3.62–3.68 (48H, m), 1.48 (18H, s), –2.76 (2H, s). MS (MALDI) m/z 1631.456 (M + H$^+$), calculated for $C_{88}H_{111}N_8O_{22}$ 1631.7735. To a solution of the Boc-protected pegylated porphyrin (0.032 g, 0.020 mmol) in 1 mL of dichloromethane was added TFA (1 mL). The reaction mixture was stirred at room temperature for 4 h and then the solvent was evaporated under vacuum to leave a green residue, which was washed with diethyl ether to remove traces of TFA and then dried under vacuum to give 0.0.028 g, 95% yield. UV-Vis (MeOH) λ_{max} (ε/M^{-1}cm^{-1}) 421 (128 300), 517 (9900), 554 (6300), 591 (4000), 647 (3 400). ^{1}H NMR ($CDCl_3$, 300 MHz): δ 8.58–8.61 (16H, m), 8.39 (4H, s), 7.96–8.01 (8H, m), 7.75 (2H, s br), 4.41 (4H, s), 4.33 (4H, s), 4.04 (4H, s), 3.66–3.69 (48H, m). The dipegylated porphyrin (0.0065 g, 0.00427 mmol) was dissolved in 1 mL of DMF and to this solution were added Et_3N (0.000 95 g, 0.009 394 mmol), HOBt (0.001 43 g, 0.009 394 mmol), DMAP (0.0011 g, 0.000 93 mmol), HGlyProLys(Boc)Lys(Boc)Lys(Boc)Arg(Pbf)Lys(Boc)Val(O^{t}Bu) (0.015 49 g, 0.009 394 mmol), and EDCI (0.018 g, 0.009 394 mmol). The reaction mixture was stirred at room temperature for 48 h. Reaction work-up was performed as described above. The porphyrin-protected peptide conjugate was isolated by flash chromatography on silica gel using $CHCl_3$–MeOH 9 : 1 and 8 : 2 for elution, giving 0.076 g, 38% yield. ^{1}H NMR ($CDCl_3$, 300 MHz): δ 8.85 (8H, s), 8.17–8.22 (8H, m), 8.01–8.10 (4H, m), 7.58–7.68 (8H, m), 4.37 (4H, s), 4.30 (4H, s), 4.00 (4H, s), 3.60–3.68 (54H, m), 2.93–3.11 (18H, m), 2.58 (4H, s), 2.51 (4H, s), 0.7–1.84 (242H, m), –2.83 (2H, s). The porphyrin-protected peptide conjugate (0.007 g, 0.0014 mmol) was dissolved in 2 mL of a mixture TFA–TIS–H_2O–phenol 88 : 2 : 5 : 5. The reaction mixture was stirred at room temperature for 4 h, then the solvent was evaporated under vacuum to leave a green oily residue. The deprotected conjugate was precipitated by the addition of Et_2O. The green precipitate was washed with Et_2O (5 × 10 mL) and then dried under vacuum giving 0.0045 g, 97% yield of **6**. UV-Vis (MeOH) λ_{max} (ε/M^{-1}cm^{-1}) 416 (326 380), 513 (15 200), 549 (10 000), 589 (7000), 646 (6000). ^{1}H NMR (D_2O, 300 MHz): δ 8.67 (4H, s), 8.27 (4H, s), 8.11 (4H, s), 4.40 (4H, s), 4.27 (12H, s, br), 4.15 (4H, s), 3.95 (9H, s), 3.95 (4H, s), 3.54–3.75 (60H, m), 3.11–3.19 (6h, m), 2.99 (20H, s), 1.27–2.00 (74H, m), 0.87–0.89 (12H, m). MS (MALDI) m/z 3366.528 (M + H$^+$) calculated for $C_{164}H_{253}N_{38}O_{38}$ 3364.9875.

Porphyrin–NLS 8 and 9. The 5,10,15,20-tetra(4-aminophenyl)porphyrin **7** (0.050 g, 0.0749 mmol) and glutaric anhydride (0.0676 g, 0.596 mmol) were dissolved in 1 mL of DMF.[26] The mixture was stirred overnight at room temperature, diluted with ethyl acetate and the target compound precipitated by the addition of hexanes. The green residue was washed with warm water to remove unreacted glutaric anhydride and then dried under vacuum to give a green solid in 0.084 g, 100% yield. ^{1}H NMR (d_6-acetone, 250 MHz): δ 10.62 (4H, s), 9.54 (4H, s), 8.91 (8H, s), 8.14 (16H, s), 2.60–2.66 (2H, m), 2.48–2.54 (2H, m, 2.09–2.14 (2H, m), –2.73 (2H, s). HRMS (MALDI) m/z 1131.4307 (M + H) calculated for $C_{64}H_{58}N_8O_{12}$ 1131.4252. The tetra-carboxylated porphyrin (0.010 g, 0.00884 mmol) was conjugated to the protected peptide sequence HGlyProLys(Boc)Lys(Boc)Lys(Boc)Arg(Pbf)Lys(Boc)Val(O^{t}Bu) (0.07289 g, 0.0442 mmol) using the same procedure as described above for conjugate **6**. Two fractions were isolated by flash chromatography using $CHCl_3$–CH_3OH 9 : 1 and 8 : 2 for elution. Deprotection of the peptide sequence for each fraction was performed as described above using a mixture of TFA–TIS–H_2O–phenol 88 : 2 : 5 : 5. The first fraction was identified by MS (MALDI) as conjugate **9** showing m/z 3916.92 (M + Na$^+$),

calculated for $C_{190}H_{295}N_{53}O_{36}Na$ 3918.2882, obtained in 31% yield. The second fraction was identified as conjugate **8**, MS (MALDI) *m/z* 4815.61 (M^+) calculated for $C_{232}H_{374}N_{68}O_{44}$ 4816.9118, obtained in 37% yield. The purity of the conjugate was 96% as determined by HPLC on an analytical Delta Pak C_{18} (3.9 × 150 mm, 5 μm) column, $t_r = 9.31$ min. For porphyrin–NLS conjugate **8**: UV-Vis (MeOH) λ_{max} ($\varepsilon/M^{-1}cm^{-1}$) 420 (246 100), 516 (12 700), 552 (10 000), 592 (5700), 650 (7200). ^1H NMR (d_6-DMSO, 300 MHz): δ 8.85 (7H, s), 8.09 (31H, s), 7.77 (42H, m), 7.08 (10H, s, br), 4.25 (10H, s), 3.05 (16H, s), 2.32 (12H, s), 1.94 (24H, s), 1.51 (72H, s), 1.30 (12H, s), 0.86 (24H, s), –2.90 (2H, s). For porphyrin–NLS conjugate **9**: the purity of the conjugate was 92% as determined by HPLC on an analytical Delta Pak C_{18} (3.9 × 150 mm, 5 μm) column, $t_r = 4.11$ min. UV-Vis (MeOH) λ_{max} ($\varepsilon/M^{-1}cm^{-1}$) 420 (301 300), 516 (16 800), 552 (13 700), 591 (8600), 650 (10 100). ^1H NMR (d_6-DMSO, 300 MHz): δ 10.41 (1H, s), 8.86 (5H, s), 7.97–8.41 (34H, m), 7.80 (24H, s), 7.24 (5H, s, br), 4.14–4.25 (16H, m), 3.94 (4H, s), 3.46 (48H, s, br), 3.07 (9H, s), 2.74 (18H, s), 2.32 (7H, s), 1.93-2.04 (14H, m), 1.32–1.51 (70H, m), 0.86 (18H, s), –2.9 (2H, s).

Porphyrin–NLS 10. The 5,10,15,20-tetra(p-aminophenyl)-porphyrin **7** (0.020 g, 0.030 mmol) and glycolic anhydride (0.032 g, 0.240 mmol) were dissolved in 1 mL of DMF. The reaction mixture was stirred at room temperature overnight, then diluted with 10 mL of $CHCl_3$, followed by addition of hexanes until precipitation occurred. The precipitate was filtered and washed with water to remove residual anhydride, and then dried under vacuum. The tetra-carboxylated porphyrin was obtained in 95% yield (0.032 g). UV-Vis (CH_3OH) λ_{max} ($\varepsilon/M^{-1}cm^{-1}$) 418 (407 300), 515 (16 100), 551 (11 500), 591 (5800), 648 (6200). ^1H NMR (DMSO-d_6, 300 MHz): δ 10.35 (4H, s), 8.84–8.87 (6H, m), 8.02–8.12 (12H. m), 4.31–4.33 (16H, m), –2.92 (2H, s). MS (MALDI) *m/z* 1138.561 (M^+), calculated for $C_{60}H_{50}N_8O_{16}$ 1138.3345. The tetracarboxylated porphyrin (0.019 g, 0.017 mmol) was dissolved in DMF (1 mL) and to this solution were added Et_3N (0.010 g, 0.102 mmol) and HOBt (0.015 g, 0.102 mmol). After stirring the mixture for 5 min $NH_2CH_2CH_2(OCH_2CH_2)_5OCH_2CO_2{}^tBu$ (0.041 g, 0.105 mmol) was added followed by EDCI (0.019 g, 0.102 mmol) and stirring continued for 48 h at room temperature. The reaction mixture was diluted with 50 mL of ethyl acetate, washed with water (3 × 100 mL), dried over anhydrous Na_2SO_4, and the solvent evaporated under vacuum. The Boc-protected pegylated porphyrin was purified by flash chromatography on silica gel using ethyl acetate followed by ethyl acetate–methanol 9 : 1 for elution. The *tert*-butyl ester precursor was obtained in 40% yield (0.018 g). UV-Vis ($CHCl_3$) λ_{max} ($\varepsilon/M^{-1}cm^{-1}$) 423 (394 100), 519 (16 300), 555 (11 800), 592 (6500), 647 (6600). ^1H NMR ($CDCl_3$, 300 MHz): δ 8.86 (6H, s), 8.16–8.19 (6H, m), 8.07–8.10 (6H, m), 7.46 (4H, s), 4.37 (8H, s), 4.16 (8H, s), 3.98 (8H, s), 3.52–3.67 (100H, m), –2.77 (2H, s). MS (MALDI) *m/z* 2646.42 (M + H^+), calculated for $C_{132}H_{190}N_{12}O_{44}$ 2647.2999. Removal of the *tert*-butyl group was achieved by dissolving the *tert*-butyl ester in a mixture of CH_2Cl_2–TFA 1 : 1. The mixture was stirred at room temperature for 4 h. After removal of the solvent under vacuum, the residue was triturated, washed with diethyl ether and dried under vacuum to give the carboxylated pegylated porphyrin in quantitative yield. (0.015 g). UV-Vis ($CHCl_3$) λ_{max} ($\varepsilon/M^{-1}cm^{-1}$) 424 (351 100), 518 (18 700), 555 (16 500), 593 (9800), 650 (10 000). ^1H NMR ($CDCl_3$, 300 MHz): δ 10.06 (4H, s), 8.54 (16H, s), 8.35–8.38 (8H, m), 7.77 (4H, s), 4.37 (8H, s), 4.29 (8H, s), 4.14 (8H, s), 3.68–3.57 (100H, m). MS (MALDI) *m/z* 2424.047 (M^+), calculated for $C_{116}H_{158}N_{12}O_{44}$ 2424.5497. Conjugation of the tetra-pegylated porphyrin (0.028 g, 0.01146 mmol) to the protected peptide HGlyProLys(Boc)Lys(Boc)Lys(Boc)Arg(Pbf)Lys(Boc)Val(O^{t}Bu) (0.0945 g, 0.0573 mmol) was performed as described above for conjugate **6**. The protected conjugate was isolated by flash chromatography on silica gel using $CHCl_3$–CH_3OH 9 : 1 for elution giving 0.0537 g, 52% yield. UV-Vis ($CHCl_3$) λ_{max} ($\varepsilon/M^{-1}cm^{-1}$) 423 (325 600), 518 (14 300), 55 (11 700), 591 (8200), 649 (7500). Deprotection of the peptide sequence was achieved as described above for conjugate **6** yielding 0.0293 g 86% of conjugate **10**. UV-Vis (MeOH) λ_{max} ($\varepsilon/M^{-1}cm^{-1}$) 420 (250 800), 516 (11 600), 552 (9500), 590 (6500), 648 (6000). H NMR (d_6-DMSO, 300 MHz): δ 10.53 (2H, s), 8.87 (4H, s), 7.80–8.15 (78H, m), 7.39 (10H, s), 4.20–4.46 (30H, m), 3.92 (20H, s), 3.33–3.5 (154H, m), 3.05 (8H, s), 2.74 (26H, s), 1.09–2.02 (114H, m), 0.85 (24H, s), –2.90 (2H, s). MS (MALDI) *m/z* (M^{+3}) 2037.57, (M^+) calculated for $C_{284}H_{474}N_{72}O_{76}$ 6113.24, (M^{+3}) 2038.74.

CD studies

The CD measurements were carried out on a AVIV 620S Circular Dichroism Spectrometer, using 1 mm path length quartz cells. 20 μM Porphyrin–peptide conjugate solutions were prepared at room temperature in water–TFE 9 : 1, pH 7.00. All spectra correspond to an average of three separate experiments and were corrected by the base line obtained for porphyrin–peptide conjugate free solutions.

Cell studies

All tissue culture media and reagents were obtained from Invitrogen. Human HEp2 cells were obtained from ATCC and maintained in a 50 : 50 mixture of DMEM–Advanced MEM containing 5% FBS. The cells were subcultured biweekly to maintain sub-confluent stocks.

For the time-dependent experiments, HEp2 cells were plated at 10 000 per well in a Costar 96 well plate and allowed to grow for 36 h. Porphyrin stocks were prepared in DMSO or water at a concentration of 10 mM and then diluted into medium to final working concentrations. The cells were exposed to 10 μM of each conjugate for 0, 1, 2, 4, 8, and 24 h. At the end of the incubation time the loading medium was removed and the cells were washed with PBS. Intrinsic fluorescence of the porphyrin was used to determine the porphyrin concentration, by reading the red emission at 650 nm after excitation at 410 nm using a BMG FLUOstar plate reader. The cell numbers were quantified by measuring cellular DNA concentration using the fluorescent CyQuant reagent (Molecular Probes).

For the dark cytotoxicity experiments the HEp2 cells were plated as described above and allowed 36–48 h to attach. The cells were exposed to increasing concentrations of porphyrin up to 100 μM and incubated overnight. The cell viability was measured using Promega's Cell Titer Blue assay reagent. Briefly, the loading medium was then removed and the cells fed medium containing Cell Titer Blue (Promega) as per manufacturer's instructions.

Viable cells convert the assay substrate to a fluorescent product that can then be measured spectroscopically. Cell toxicity was determined by reading the fluorescence at 520/584 nm (excitation/emission) using a BMG FLUOstar plate reader. The signal was normalized to 100% viable (untreated) cells and 0% viable (treated with 0.2% saponin from Sigma) cells.

For the phototoxicity experiments, the HEp2 cells were prepared as described above for the dark cytotoxicity assay and treated with porphyrin concentrations of 0, 0.625, 1.25, 2.5, 5, and 10 μM. After compound loading, the medium was removed and replaced with medium containing 50 mM HEPES pH 7.4. The cells were then placed on ice and exposed to light from a 100 W halogen lamp filtered through a 610 nm long pass filter (Chroma) for 20 min. An inverted plate lid filled with water to a depth of 5 mm acted as an IR filter. The total light dose was approximately 0.5 J cm^{-2}. The cells were returned to the incubator for 24 h after which, cell viability was measured as described for the dark toxicity assay.

For the microscopy experiments the HEp2 cells were plated on LabTek 2 chamber coverslips and incubated overnight, followed by an overnight loading using 10 μM of porphyrin. Natural fluorescence of the porphyrin macrocycle occurs in the red region of the optical spectrum. This allows use of standard Texas Red fluorescent filter sets to visualize the intercellular localization of the porphyrins. To visualize specific cellular compartments, cells were stained for 30 min with the following organelle stains (from Molecular Probes, as per manufacturers instructions) after preloading the cells with porphyrin: Mitochondria: MitoTracker Green at 250 nM, Lysosomes: LysoSensor Green at 50 nM, Endoplasmic Reticulum (ER): ERtracker Blue-White at 100 nM or $DiOC_6$ (Molecular Probes) at 5 μg mL^{-1}. The slides were washed three times with growth medium and new medium containing 50 mM HEPES pH 7.4 was added. By utilizing green fluorescing organelle tracers, it becomes possible to identify the intracellular compartments associated with the porphyrins; when the red and green images are overlaid, areas of co-localization appear as orange-yellow regions. Fluorescent microscopy was performed using a Zeiss Axiovert 200M inverted fluorescent microscope fitted with standard FITC and Texas Red filter sets (Chroma). The images were acquired with a Zeiss Axiocam MRM CCD camera fitted to the microscope.

Acknowledgements

The authors thank Ms Martha Juban for the synthesis of the linear peptide. This work was partially supported by the National Science Foundation, grant number CHE-304833.

Notes and references

1 T. J. Dougherty, C. J. Gomer, B. W. Henderson, G. Jori, D. Kessel, M. Korbelik, J. Moan and Q Peng, *J. Natl. Cancer Inst.*, 1998, **90**, 889–905.
2 R. K. Pandey and G. Zheng, G, *The Porphyrin Handbook*, K. M. Kadish, K. M. Smith and R. Guilard, ed., Academic Press, Boston, MA, 2000, 6, pp. 157-230.
3 M. F. Hawthorne, *Angew. Chem., Int. Ed. Engl.*, 1993, **32**, 950–984.
4 A. H. Soloway, W. Tjarks, B. A. Barnum, F. G. Rong, R. F. Barth, I. M. Codogni and J. G. Wilson, *Chem. Rev.*, 1998, **98**, 1515–1562.
5 R. F. Barth, J. A. Coderre, M. G. H. Vicente and T. E. Blue, *Clin. Cancer Res.*, 2005, **11**, 3987–4002.
6 J. Osterloh and M. G. H. Vicente, *J. Porphyrins Phthalocyanines*, 2002, **6**, 305–324.
7 W. M. Sharman, J. E. van Lier and C. M. Allen, *Adv. Drug Delivery Rev.*, 2004, **56**, 53–76.
8 R. Hudson and R. W. Boyle, *J. Porphyrins Phthalocyanines*, 2004, **8**, 954–975.
9 T. Boulikas, *Critical Reviews Eukar. Gene Exp.*, 1993, **3**, 193–227.
10 E. Lombardo, J. C. Ramirez, J. Garcia and J. M. Almendral, *J. Virol.*, 2002, **76**, 7049–7059.
11 D. Kalderon, B. L. Roberts, W. D. Richardson and A. E. Smith, *Cell*, 1984, **39**, 499–509.
12 R. E. Lanford and J. S. Butel, *Cell*, 1984, **37**, 801–813.
13 R. E. Lanford, P. Kanda and R. C. Kennedy, *Cell*, 1986, **46**, 575–582.
14 C. M. Feldherr, R. E. Lanford and D. Akin, *Proc. Natl. Acad. Sci. U. S. A.*, 1992, **89**, 11002–11005.
15 L. Chaloin, P. Bigey, C. Loup, M. Marin, N. Galeotti, M. Piechaczyk, F. Heitz and B. Meunier, *Bioconjugate Chem.*, 2001, **12**, 691–700.
16 S. K. Bisland, D. Singh and J. Gariepy, *Bioconjugate Chem.*, 1999, **10**, 982–99.
17 A. S. Sobolev, T. V. Akhlynina, S. V. Yachmenev, A. A. Rosenkranz and E. S. Severin, *Biochem. Int.*, 1992, **26**, 445–450.
18 T. V. Akhlynina, A. A. Rosenkranz, D. A. Jans, P. V. Gulak, N. V. Serebryakova and A. S. Sobolev, *Photochem. Photobiol.*, 1993, **58**, 45–48.
19 T. V. Akhlynina, D. A. Jans, A. A. Rosenkranz, N. V. Statsyuk, I. Y. Balashova, G. Toth, I. Pavo, A. B. Rubin and A. S. Sobolev, *J. Biol. Chem.*, 1997, **272**, 20328–20331.
20 T. V. Akhlynina, D. A. Jans, N. V. Statsyuk, I. Y. Balashova, G. Toth, I. Pavo, A. A. Rosenkranz, B. S. Naroditsky and A. S. Sobolev, *Int. J. Cancer*, 1999, **81**, 734–740.
21 M. Sibrian-Vazquez, T. J. Jensen, R. P. Hammer and M. G. H. Vicente, *J. Med. Chem.*, 2006, **49**, 1364–1372.
22 M. Sibrian-Vazquez, T. J. Jensen and M. G. H. Vicente, *J. Med. Chem.*, 2008, **51**, 2915–2923.
23 I. Sehgal, M. Sibrian-Vazquez and M. G. H. Vicente, *J. Med. Chem.*, 2008, **51**, 6014–6020.
24 M. Sibrian-Vazquez, T. J. Jensen and M. G. H. Vicente, *J. Photochem. Photobiol., B*, 2007, **86**, 9–21.
25 R. Luguya, L. Jaquinod, F. R. Fronczek, M. G. H. Vicente and K. M. Smith, *Tetrahedron*, 2004, **60**, 2757–2763.
26 M. Sibrian-Vazquez, T. J. Jensen, F. R. Fronczek, R. P. Hammer and M. G. H. Vicente, *Bioconjugate Chem.*, 2005, **16**, 852–863.
27 N. Greenfield and G. D. Fasman, *Biochemistry*, 1969, **8**, 4108–4116.
28 E. Conti, M. Uy, L. Leighton, G. Blobel and J. Kuriyan, *Cell*, 1998, **94**, 193–204.
29 B. W. Henderson, D. A. Bellnier, W. R. Greco, A. Sharma, R. K. Pandey, L. A. Vaughan, K. R. Weishaupt and T. J. Dougherty, *Cancer Res.*, 1997, **57**, 4000–4007.
30 S.-A. Cryan, *AAPS J.*, 2005, **7**, E20–E41.
31 D. Kessel, *J. Porphyrins Phthalocyanines*, 2004, **8**, 1009–1014.
32 S. I. Dworetzky, R. E. Lanford and C. M. Feldherr, *J. Cell Biol.*, 1988, **107**, 1279–1287.
33 Y. Ye, S. Bloch, B. Xu and S. Achilefu, *J. Med. Chem.*, 2006, **49**, 2268–2275.
34 H. D. Maynard, S. Y. Okada and R. H. Grubbs, *J. Am. Chem. Soc.*, 2001, **123**, 1275–1279.
35 R. J. Kok, A. J. Schraa, E. J. Bos, H. E. Moorlag, S. A. Asgeirsdottir, M. Everts, D. K. F. Meijer and G. Molema, *Bioconjugate Chem.*, 2002, **13**, 128–135.
36 G. Thumshirn, U. Hersel, S. L. Goodman and H. Kessler, *Chem.–Eur. J.*, 2003, **9**, 2717–2725.
37 D. Boturyn, J.-L. Coll, E. Garanger, M.-C. Favrot and P. Dumy, *J. Am. Chem. Soc.*, 2004, **126**, 5730–5739.
38 R. Shukla, T. P. Thomas, J. Peters, A. Kotlyar, A. Myc and J. R. Baker, *Chem. Commun.*, 2005, 5739–5741.

